The EMBO Journal (2008) 27, 1122–1133 | © 2008 European Molecular Biology Organization | All Rights Reserved 0261-4189/08
www.embojournal.org

THE EMBO JOURNAL

Chloroplast monothiol glutaredoxins as scaffold proteins for the assembly and delivery of [2Fe–2S] clusters

Sibali Bandyopadhyay[1,6], Filipe Gama[2,6], Maria Micaela Molina-Navarro[3], José Manuel Gualberto[4], Ronald Claxton[1], Sunil G Naik[5], Boi Hanh Huynh[5], Enrique Herrero[3], Jean Pierre Jacquot[2], Michael K Johnson[1,*] and Nicolas Rouhier[2,*]

[1]Department of Chemistry, Centre for Metalloenzyme Studies, University of Georgia, Athens, GA, USA, [2]UMR 1136 IaM, IFR 110, Faculté des Sciences, Nancy University, Vandoeuvre, France, [3]Department of Basic Medical Sciences, University of Lleida, Lleida, Spain, [4]Institut de Biologie Moléculaire des Plantes, CNRS, Strasbourg, France and [5]Department of Physics, Emory University, Atlanta, GA, USA

Glutaredoxins (Grxs) are small oxidoreductases that reduce disulphide bonds or protein-glutathione mixed disulphides. More than 30 distinct grx genes are expressed in higher plants, but little is currently known concerning their functional diversity. This study presents biochemical and spectroscopic evidence for incorporation of a [2Fe–2S] cluster in two heterologously expressed chloroplastic Grxs, GrxS14 and GrxS16, and *in vitro* cysteine desulphurase-mediated assembly of an identical [2Fe–2S] cluster in apo-GrxS14. These Grxs possess the same monothiol CGFS active site as yeast Grx5 and both were able to complement a yeast *grx5* mutant defective in Fe–S cluster assembly. *In vitro* kinetic studies monitored by CD spectroscopy indicate that [2Fe–2S] clusters on GrxS14 are rapidly and quantitatively transferred to apo chloroplast ferredoxin. These data demonstrate that chloroplast CGFS Grxs have the potential to function as scaffold proteins for the assembly of [2Fe–2S] clusters that can be transferred intact to physiologically relevant acceptor proteins. Alternatively, they may function in the storage and/or delivery of preformed Fe–S clusters or in the regulation of the chloroplastic Fe–S cluster assembly machinery.

The EMBO Journal (2008) **27,** 1122–1133. doi:10.1038/emboj.2008.50; Published online 20 March 2008
Subject Categories: proteins; plant biology
Keywords: chloroplast; glutaredoxin; iron–sulphur protein; plant

*Corresponding authors. N Rouhier, UMR 1136 IaM, IFR 110, Faculté des Sciences, Nancy University, Vandoeuvre 54506, France.
Tel.: +33 3 83684225; Fax: +33 3 83684292;
E-mail: nrouhier@scbiol.uhp-nancy.fr or
MK Johnson, Department of Chemistry, Centre for Metalloenzyme Studies, University of Georgia, Athens, GA, USA.
Tel.: +1 706 542 9378; Fax: + 1 706 542 9454;
E-mail: johnson@chem.uga.edu
[6]These authors contributed equally to this work

Received: 27 September 2007; accepted: 25 February 2008; published online: 20 March 2008

Introduction

Iron–sulphur (Fe–S) proteins are intimately involved in numerous essential biological processes, such as photosynthesis, respiration and the metabolism of carbon, oxygen, hydrogen, nitrogen and sulphur (Johnson and Smith, 2005). However, little is known concerning the mechanism of Fe–S cluster biogenesis in plants. Much of the current understanding of Fe–S cluster biogenesis stems from investigation of components of the bacterial *isc* (iron–sulphur cluster assembly), *suf* (sulfur mobilization) and *nif* (nitrogen fixation) operons (Johnson *et al*, 2005) and identification and characterization of homologous ISC-type proteins in yeast and mammalian mitochondria (Lill and Mühlenhoff, 2005). The ISC, SUF and NIF Fe–S cluster assembly machineries share a common basic mechanism involving cysteine desulphurase (IscS, SufS and NifS)-mediated assembly of [2Fe–2S] or [4Fe–4S] clusters on U-type (IscU, SufU and N-terminal domain of NifU), A-type (IscA, SufA and ^{Nif}IscA) and Nfu-type (corresponding to the C-terminal domain of NifU) scaffold proteins, and subsequent intact cluster transfer into acceptor apo-proteins. In the case of the ISC machinery, [2Fe–2S] cluster transfer from IscU is facilitated by specific molecular co-chaperones (HscA and HscB) in an ATP-dependent reaction (Chandramouli and Johnson, 2006) and [4Fe–4S] cluster assembly on dimeric IscU occurs at the subunit interface via reductive coupling of two [2Fe–2S] clusters (Chandramouli *et al*, 2007). However, little is currently known concerning the detailed mechanism of Fe–S cluster assembly and transfer involving scaffold proteins. In plants, Fe–S cluster biosynthesis primarily occurs in mitochondria, using the ISC machinery with Isu, IscA and Nfu as potential scaffold proteins, and in chloroplasts using the SUF machinery with SufA, SufB and Nfu proteins as potential scaffold proteins (Balk and Lobreaux, 2005; Ye *et al*, 2006b; Layer *et al*, 2007).

Glutaredoxins (Grxs) are small proteins that normally function in the reduction of disulphide bridges or glutathionylated proteins. However, recent studies in *Saccharomyces cerevisiae* and *Escherichia coli* have indicated specific roles for some Grxs in facilitating Fe–S cluster biosynthesis (Rodríguez-Manzaneque *et al*, 2002; Mühlenhoff *et al*, 2003; Achebach *et al*, 2004). Yeast cells deleted for the *GRX5* gene were found to be more sensitive to oxidative stress, to accumulate free iron and to have impaired mitochondrial Fe–S cluster biogenesis and respiratory growth (Rodríguez-Manzaneque *et al*, 1999, 2002). Other prokaryotic and eukaryotic CGFS Grxs have been shown to be efficient functional substitutes for yeast Grx5 (Cheng *et al*, 2006; Molina-Navarro *et al*, 2006). Although the specific function of yeast Grx5 in Fe–S cluster biogenesis remains to be elucidated, ^{55}Fe radiolabelling studies of knockout mutants implicate a role in mediating transfer of clusters preassembled on the Iscu1p scaffold protein into acceptor

proteins (Mühlenhoff *et al*, 2003). The discovery that Grx5 is also required for vertebrate haem synthesis raises the possibility that Grx5 is a key determinant for channelling Fe into haem and Fe–S cluster biosynthesis in mammals (Wingert *et al*, 2005).

The most obvious role for Grxs in Fe–S cluster biogenesis lies in facilitating Fe–S cluster assembly or transfer by reducing disulphides on scaffold or apo forms of Fe–S proteins. However, the discovery that some Grxs can assemble Fe–S clusters suggests the possibility of alternative roles in Fe–S cluster assembly or transfer. Poplar GrxC1 (CGYC active site) and human Grx2 (CSYS active site) are homodimers with a subunit-bridging [2Fe–2S] cluster ligated by one active site cysteine of each monomer and the cysteines of two external glutathione (GSH) molecules (Feng *et al*, 2006; Johansson *et al*, 2007; Rouhier *et al*, 2007). The cluster-containing dimeric form of human Grx2 was proposed to function as a redox sensor for the activation of Grx2 in case of oxidative stress (Lillig *et al*, 2005). Although this is a viable hypothesis, mutagenesis studies on poplar GrxC1 indicate that incorporation of a [2Fe–2S] cluster is likely to be a general feature of plant Grxs possessing a glycine adjacent to the catalytic cysteine (Rouhier *et al*, 2007). Hence CGFS Grxs, such as yeast Grx5, might have the capacity to incorporate a Fe–S cluster. Moreover, the requirement of GSH for the export of a Fe–S cluster (or a precursor thereof) from mitochondria to facilitate the assembly of cytosolic Fe–S proteins in *S. cerevisiae* (Lill and Mühlenhoff, 2005) provides further circumstantial evidence in support of a role for GSH- and Grx-ligated [2Fe–2S] clusters in Fe–S biogenesis.

In higher plants, around 30 different Grx isoforms can be classified into three distinct subgroups depending on their active site sequences (Rouhier *et al*, 2004). The first class, which contains Grxs with C[P/G/S][Y/F][C/S] motifs other than CGFS, is homologous to the classical dithiol Grxs such as *E. coli* Grx1 and 3, yeast Grx1 and 2 and mammalian Grx1 and 2. The second class has a strictly conserved CGFS active site sequence and includes Grxs homologous to yeast Grx3, 4 and 5 or *E. coli* Grx4. Plants have generally four members in this group (GrxS14 to S17). The properties of proteins of the third class, which is specific to higher plants and involves a CC[M/L][C/S] active site, are largely unknown.

This study presents biochemical, spectroscopic and analytical evidence for the incorporation of [2Fe–2S] clusters in two plant chloroplast CGFS Grxs, GrxS14 and S16, and both *in vivo* and *in vitro* evidence for their involvement in the maturation of Fe–S proteins. The results demonstrate that monothiol Grxs have the potential to function as scaffold proteins for *de novo* synthesis and efficient delivery of [2Fe–2S] clusters, as Fe–S cluster delivery or storage proteins for mediating the transfer of Fe–S clusters from ISC or SUF scaffold proteins to acceptor proteins, or as sensors of the cellular Fe–S cluster status in Fe homoeostasis.

Results

The plant CGFS Grx subgroup

In silico analysis of Grxs from different kingdoms reveals that four or five Grxs with CGFS active site are generally present in higher plants and in *Chlamydomonas reinhardtii*, whereas only three are present in *S. cerevisiae*, two in most other fungi and in mammals, one in *Synechocystis* and in *E. coli* (Rouhier *et al*, 2004). In *Populus trichocarpa*, GrxS14 and S15 are small proteins (171 and 172 amino acids, respectively, including the transit peptide sequence) with a single repeat of the Grx module. GrxS16 is larger (296 amino acids including the transit peptide sequence) with an N-terminal extension linked to the Grx module. GrxS17 is larger (492 amino acids) and displays an N-terminal Trx-like domain with a WCDAS active site followed by three successive Grx modules. A careful examination of amino-acid sequence alignments (Supplementary Figure 1) indicates that although not present in all CGFS Grxs, a second cysteine is found in 60% of the 250 CGFS Grxs found in GenBank at a conserved position closer to the C terminus. It is conserved in GrxS14 and S16 (Cys 87 in GrxS14 and Cys 221 in GrxS16, numbering based on the recombinant mature protein sequences), in the third module of GrxS17 and in GrxC1, whereas it is absent in GrxS15, in the second Grx domain of GrxS17 and in GrxC4 and only partly conserved in the first Grx domain of plant GrxS17. In *Sc*Grx5, these two cysteines are able to form a disulphide bridge in the presence of oxidized GSH (Tamarit *et al*, 2003).

Subcellular localization of the CGFS Grxs

We have determined the localization of all the CGFS Grxs that possess an N-terminal transit sequence. GrxS17, predicted to be cytosolic, does not seem to possess such an extension and its localization has not been characterized further. The full-length sequences of the three other Grxs devoid of the stop codon were introduced in frame before the GFP sequence and the construction was used to bombard tobacco leaves. As shown in Figure 1, the fluorescence of GrxS14 and S16 strictly coincides with the one of the chlorophyll, whereas the fluorescence of GrxS15 superimposed well with one of the mitochondrial marker. Therefore, GrxS14 and S16 are chloroplastic and GrxS15 is mitochondrial.

Some poplar monothiol but not dithiol Grxs rescue the defects of a yeast mutant lacking Grx5

To determine whether the four poplar monothiol Grxs rescue the defects of a *yeast* Δ*grx5* mutant, we targeted the proteins at the mitochondrial matrix (Molina *et al*, 2004). All the proteins were adequately compartmentalized in the mitochondrial matrix (Figure 2A). Of the two poplar Grxs with a single Grx domain, GrxS14 and S15, only the first one rescued the *grx5* mutant defects in respiratory growth (Figure 2B) and its sensitivity to oxidants (Figure 2C). These defects were also efficiently rescued by GrxS16 and S17. To test whether a single Grx domain is sufficient for the function of GrxS17, we fused only the most C-terminal domain of S17 (from amino acid 398 to 492) to the mitochondrial targeting sequence of Grx5 ($S17_{398-492}$). This protein was also compartmentalized at the mitochondrial matrix (Figure 2A), although a double band appeared. The band with lower mobility probably corresponds to unprocessed precursor still compartmentalizing at yeast mitochondria. $S17_{398-492}$ suppressed partially the growth phenotypes of the *grx5* mutant, in particular growth in respiratory conditions (Figure 2B). The ratio of activities of the mitochondrial enzymes aconitase (containing Fe–S clusters) and malate dehydrogenase (without Fe–S clusters) was used as a measure of the efficiency of the Fe–S cluster assembly in mitochondrial proteins (Molina *et al*, 2004). This ratio was measured in strains carrying all these constructions in a chromosomal *grx5* back-

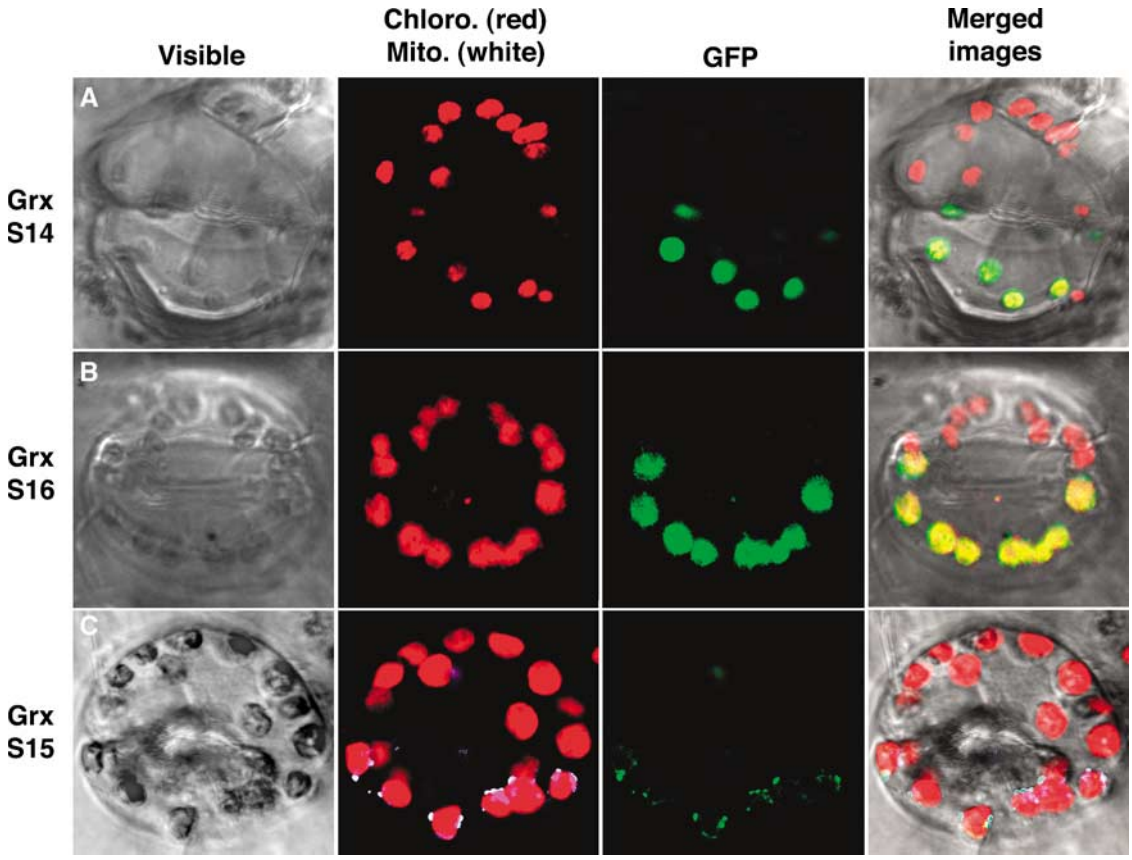

Figure 1 Subcellular localization of CGFS Grxs by GFP fusion. (**A**) GrxS14, (**B**) GrxS16 and (**C**) GrxS15. From left to right: visible light, autofluorescence of chlorophyll (red) or mitochondrial marker (white); fluorescence of the constructions and merged images. Only one of the guard cells shows chloroplast-localized GFP, because a small numbers of cells were transfected. As the mitochondrial marker (DsRed) is co-transfected with the GFP construction, it is only visible in the cell that expresses GFP.

ground (Figure 2D). Ratios were comparable with wild type in strains expressing the mitochondrial forms of S14, S16 and S17, in accordance with the growth phenotypes. In contrast, both S15 and the truncated form of S17 exhibited much lower enzyme ratios (Figure 2D). For all the strains tested, absolute malate dehydrogenase levels were basically similar, and doxycycline addition to growth media lowered aconitase activity to basal levels (data not shown). For the monothiol Grxs analysed, there appears to be a correlation between efficiency to express active aconitase and growth phenotypes, except that poplar mitochondrial S15 did not rescue at all the growth defects of the yeast mutant, although still being able to synthesize low levels of mature aconitase. The anomalous results with S15 and $S17_{398-492}$ are puzzling and may indicate functional diversity within the general class of monothiol Grxs (see below) or that aconitase maturation does not provide a good measure of the efficiency of general Fe–S cluster biosynthesis in mitochondria. The latter is supported by a very recent study of the requirements for mitochondrial aconitase Fe–S cluster maturation in *S. cerevisiae*, which indicated a specific requirement for Isa1p, Isa2p and the Iba57, proteins that are not required for general Fe–S cluster biogenesis in mitochondria (Gelling *et al*, 2008).

To determine whether the capacity to bind a Fe–S cluster is sufficient for *grx5* complementation, we then used poplar GrxC1 (CGYC), which incorporates a [2Fe–2S] centre and GrxC1 G32P (CPYC) and GrxC4 (CPYC) which do not (Rouhier *et al*, 2007). Although all these Grxs were targeted to the matrix (Figure 3A), none of these proteins rescued (i) the inability of a *grx5* mutant for respiratory growth, (ii) the sensitivity to oxidants and (iii) the capacity to assembly a Fe–S cluster in aconitase (Figure 3B–D). None of the three dithiol Grxs, even the one binding a Fe–S cluster, is functional in yeast mitochondria for the maturation of Fe–S proteins. To determine whether this is caused by structural incompatibility of the dithiol Grxs with the Fe–S cluster biosynthetic machinery or more specifically by the different active site sequences with either dithiol or monothiol motifs, we modified the CGYC and CPYC active sites of GrxC1 and GrxC4 into CGFS to mimic the active site sequence of Grx5. The resulting GrxC1 CGFS fully substituted for yeast Grx5 with respect to all phenotypes analysed (Figure 3), whereas GrxC4 CGFS did not (data not shown). The GrxC1 CGFS rescuing effects did not occur when its expression from the *tet* promoter was switched off by doxycycline addition to the growth medium (data not shown). We therefore conclude that the requirement for a monothiol Grx active site could preclude poplar dithiol Grxs from functionally rescuing a *grx5* mutant, but in some cases, exemplified by the GrxC4 CGFS derivatives, other sequence or structural requirements are needed.

Purification and spectroscopic characterization of Fe–S cluster-containing poplar GrxS14 and AtGrxS16

The mature form of the three organellar poplar CGFS Grxs was expressed in *E. coli* to check their ability to incorporate

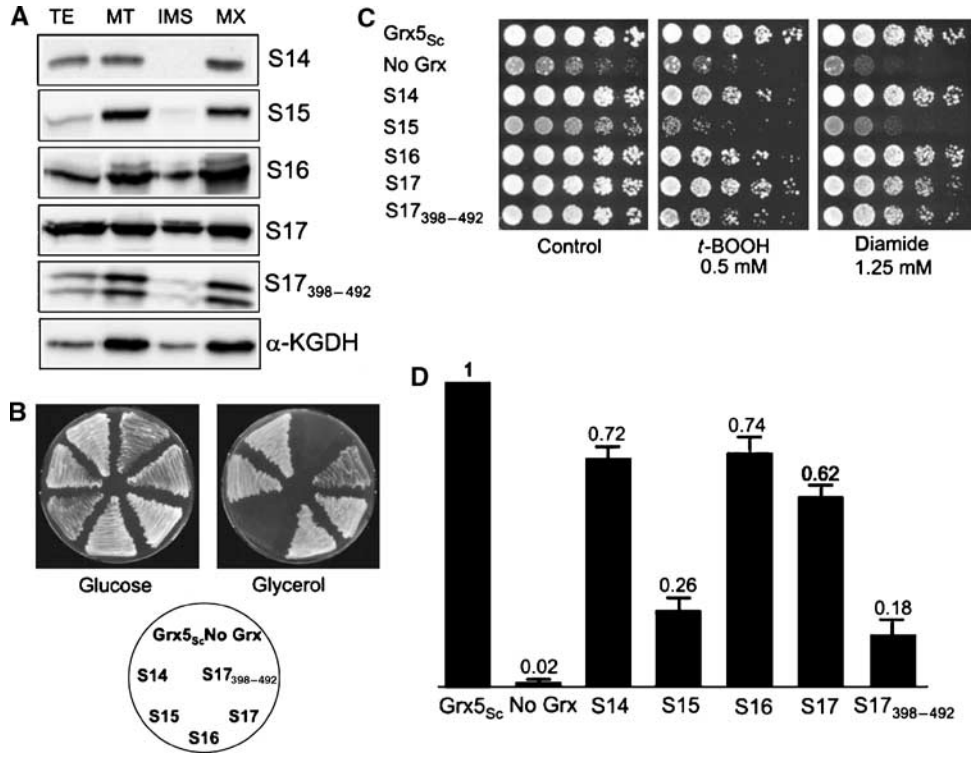

Figure 2 Rescue of the *S. cerevisiae grx5* mutant defects by poplar monothiol glutaredoxins. (**A**) Compartmentalization of GrxS14, S15, S16, S17 and $S17_{398-492}$ in the mitochondrial matrix of *S. cerevisiae* cells. Cultures were grown exponentially in YPLactate medium at 30°C to about 3×10^7 cells ml^{-1}, before mitochondrial isolation and subfractionation. TE, total cell extract; MT, mitochondrial fraction; IMS, intermembrane space; MX, matrix. Proteins (20 μg) were loaded in the TE lanes, and 5 μg was loaded in the other lanes. Anti-HA anti-lipoic acid antibodies were used in the western blot to detect the HA-tagged proteins, and the matrix marker α-ketoglutarate dehydrogenase (α-KGDH). (**B**) Growth on glucose (YPD plates) or glycerol (YPGly plates), after 3 days at 30°C. (**C**) Sensitivity to *t*-BOOH or diamide of the strains after 3 days at 30°C on YPD plates. (**D**) Ratio between aconitase and malate dehydrogenase activities in exponential cultures at 30°C in YPGalactose medium.

Fe–S clusters. On the basis of our previous experience with GrxC1, GSH, which stabilize and ligate the [2Fe–2S] cluster, was added during the first steps of the purification (Rouhier *et al*, 2007). Although the presence of a brownish colouration typical of a Fe–S cluster was clearly evident in cells overexpressing poplar and *Arabidopsis thaliana* (At) GrxS14 and S16, almost no holoprotein was obtained at the end of an aerobic purification, even in the presence of GSH, suggesting that the cluster degrades quickly in air. In contrast, there was no indication of a Fe–S cluster prosthetic group in recombinant poplar or *A. thaliana* GrxS15.

Purification of poplar GrxS14 under strictly anaerobic conditions was undertaken to address the type, stoichiometry and properties of the putative Fe–S centre. The reddish-brown purified samples contained 0.80 ± 0.10 Fe per monomer. The UV–visible absorption and CD spectra of anaerobically purified poplar GrxS14 are shown in Figure 4 and both are characteristic of a $[2Fe–2S]^{2+}$ centre (Stephens *et al*, 1978; Dailey *et al*, 1994). On the basis of the theoretical and experimental ε_{280} values for the apo protein ($9.9\,mM^{-1}\,cm^{-1}$), the ε_{280} and ε_{411} values for the $[2Fe–2S]^{2+}$ centre are estimated to be 3.9 and $4.4\,mM^{-1}\,cm^{-1}$, respectively, and the A_{411}/A_{280} was found to be 0.31 ± 0.04. In accord with the analytical data, these extinction coefficients are indicative of 0.4–0.5 $[2Fe–2S]^{2+}$ clusters per monomer. Hence the analytical, absorption and CD data are consistent with approximately one $[2Fe–2S]^{2+}$ per dimeric GrxS14. Anaerobically purified At GrxS16 contained an analogous $[2Fe–2S]^{2+}$ centre as judged by very similar UV–visible absorption and CD spectra (Figure 4).

In vitro reconstitution of aerobically purified apo GrxS14 was attempted under strictly anaerobic conditions in the presence of 5 mM GSH and 2 mM DTT, using Fe(II), L-cysteine and catalytic amounts of *E. coli* IscS. After chromatographic removal of excess reagents, the resulting cluster-loaded form of GrxS14 was essentially identical to anaerobically purified [2Fe–2S] GrxS14, as judged by Fe analyses and UV–visible absorption and CD spectra (data not shown). GSH was required for successful reconstitution of a [2Fe–2S] cluster on GrxS14. Samples of apo GrxS14 reconstituted using the same procedure in a reaction mixture containing 2 mM DTT, but no GSH, showed no evidence of the presence on a bound Fe–S cluster following repurification. Hence, *in vitro* Fe–S cluster reconstitution studies confirm the potential of poplar GrxS14 to act as a scaffold for the assembly of [2Fe–2S] clusters in a cysteine desulphurase-mediated reaction and indicate that GSH is required for cluster assembly.

Resonance Raman and Mössbauer studies of anaerobically purified poplar GrxS14 confirm the presence of a $[2Fe–2S]^{2+}$ centre and provide insight into the cluster ligation. Resonance Raman spectra obtained using 457- and 514-nm excitation reveal Fe–S stretching modes at 288, 332, 347, 365, 402 and $424\,cm^{-1}$ (Figure 5). The vibrational frequencies are generally similar to those of structurally characterized [2Fe–2S]

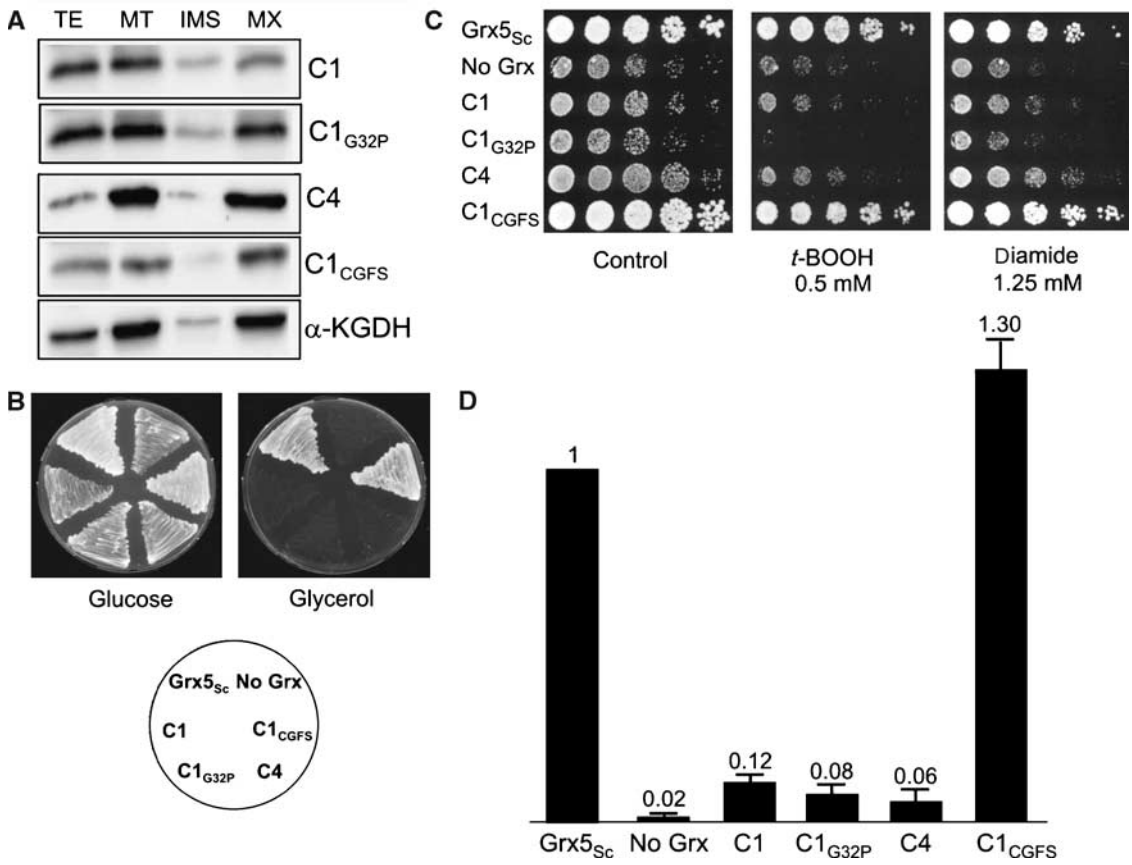

Figure 3 Rescue of the *S. cerevisiae grx5* mutant defects by poplar dithiol glutaredoxins. (**A**) Compartmentalization of GrxC1, $C1_{G32P}$, C4 and $C1_{CGFS}$ in the mitochondrial matrix of *S. cerevisiae* cells. Growth conditions and western blot analyses are similar to those described in Figure 2. TE, total cell extract; MT, mitochondrial fraction; IMS, intermembrane space; MX, matrix. (**B**) Growth on glucose (YPD plates) or glycerol (YPGly plates), after 3 days at 30°C. (**C**) Sensitivity to *t*-BOOH or diamide of the strains after 3 days at 30°C on YPD plates. (**D**) Ratio between aconitase and malate dehydrogenase activities in exponential cultures at 30°C in YPGalactose medium.

ferredoxins with complete cysteinyl cluster ligation and are readily assigned to vibrational modes of the $Fe_2S_2^bS_4^t$ unit (S^b = bridging S and S^t = terminal or cysteinyl) by direct analogy with published data (Han *et al*, 1989; Fu *et al*, 1992). Figure 6 compares the Mössbauer spectra of poplar GrxS14 with those of the all cysteinyl-ligated $[2Fe–2S]^{2+}$ cluster in poplar GrxC1 and the IscU $[2Fe–2S]^{2+}$ cluster which has one non-cysteinyl ligand (Agar *et al*, 2000). Each spectrum is indicative of a $S=0$ $[2Fe–2S]^{2+}$ centre that results from antiferromagnetic coupling of two high-spin Fe(III) ions and is simulated as the sum of quadrupole doublets from each Fe site using the parameters listed in the figure legend. The similarity and values of the isomer shift (δ) and quadrupole splitting (ΔE_Q) parameters for each Fe site of the $[2Fe–2S]^{2+}$ clusters in GrxC1 and GrxS14 are consistent with approximately tetrahedral S ligation at each Fe site. Non-cysteinyl ligation is generally manifested by anomalous isomer shifts and quadrupole splittings for the unique Fe site, which results in marked asymmetry in the observed spectrum, as is apparent in the spectrum of $[2Fe–2S]^{2+}$ centre in IscU (Agar *et al*, 2000). Hence, the Mössbauer data indicate a $[2Fe–2S]^{2+}$ cluster as the sole Fe-containing prosthetic group in anaerobically purified poplar GrxS14, and the Mössbauer and resonance Raman data taken together provide support for complete cysteinyl ligation.

Cluster ligation in GrxS14 and S16

The two structurally characterized $[2Fe–2S]^{2+}$ centres in dithiol Grxs, human Grx2 (CSYC active site) and poplar GrxC1 (CGYC active site) have very similar absorption and CD spectra and have analogous coordination environments, involving the catalytic cysteine of two Grxs and the cysteines of two GSH (Johansson *et al*, 2007; Rouhier *et al*, 2007). On the basis of UV–visible absorption and CD spectra shown in Figure 4, a distinct type of $[2Fe–2S]^{2+}$ centre may be present in GrxS14 and S16. Marked differences in the excited-state electronic properties and ground-state vibrational properties of the $[2Fe–2S]^{2+}$ centres in poplar GrxC1 and GrxS14 are evident in comparing the UV–visible absorption/CD and resonance Raman spectra shown in Figures 4 and 5, respectively. Differences in the relative intensities of corresponding Raman bands reflect changes in excitation profiles resulting from perturbation of the excited-state electronic structure. Nevertheless, it is clear that corresponding Fe–S stretching frequencies are upshifted by 2–8 cm^{-1} in GrxS14 compared with GrxC1, suggesting stronger Fe–S bonds for both terminal and bridging S.

As the spectroscopic properties of the $[2Fe–2S]^{2+}$ centres in monothiol Grxs indicate complete cysteinyl ligation, mutagenesis studies were undertaken to address the possibility that GSH is replaced as a ligand by an intrinsic cysteine

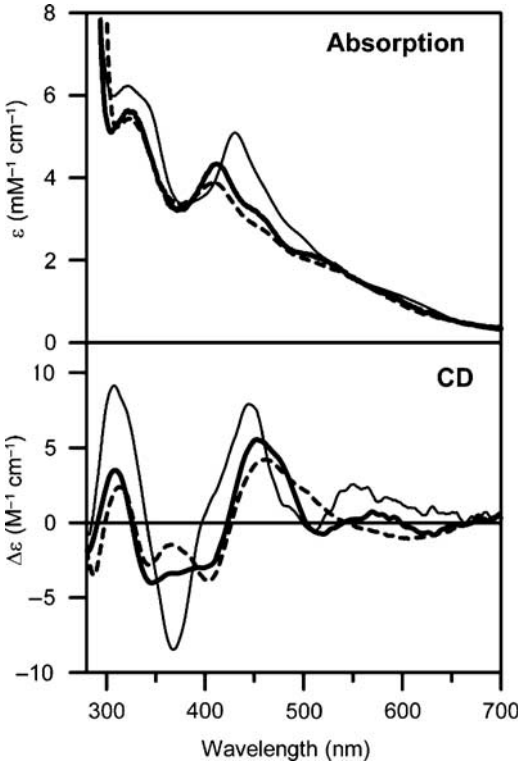

Figure 4 Comparison of the UV–visible absorption and CD spectra of [2Fe–2S] cluster-bound forms of poplar GrxS14 (thick line), At GrxS16 (broken line) and poplar GrxC1 (thin line).

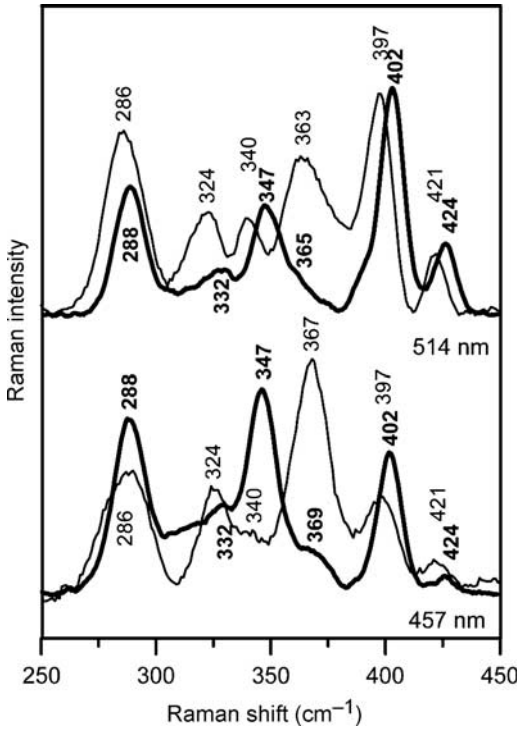

Figure 5 Comparison of the resonance Raman spectra of [2Fe–2S] cluster-bound forms of poplar GrxS14 (thick line) and GrxC1 (thin line) with 514- and 457-nm laser excitation. Samples were ~4 mM in Grx and were in the form of a frozen droplet at 17 K. Each spectrum is the sum of 100 scans, with each scan involving counting photons for 1 s each 0.5 cm^{-1} with 6 cm^{-1} spectral resolution. Lattice modes of ice have been subtracted.

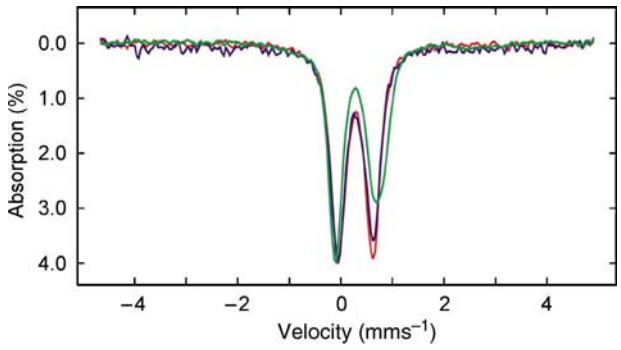

Figure 6 Comparison of the Mössbauer spectra of [2Fe–2S] cluster-bound forms of poplar GrxS14 (blue), poplar GrxC1 (red) and *A. vinelandii* IscU (green). The GrxS14 and C1 Mössbauer samples were prepared by growing cells on ^{57}Fe-enriched media and the IscU sample was prepared by IscS-mediated reconstitution using ^{57}Fe(II) (Agar *et al*, 2000). The Mössbauer spectra were recorded at 4.2 K with a magnetic field of 50 mT applied parallel to the γ-beam. Each spectrum is best simulated as the sum of two overlapping quadrupole doublets with the following parameters: $\Delta E_Q = 0.56$ and $\delta = 0.26\,mm\,s^{-1}$ for doublet 1, and $\Delta E_Q = 0.76$ and $\delta = 0.28\,mm\,s^{-1}$ for doublet 2 of GrxS14; $\Delta E_Q = 0.54$ and $\delta = 0.27\,mm\,s^{-1}$ for doublet 1, and $\Delta E_Q = 0.76$ and $\delta = 0.28\,mm\,s^{-1}$ for doublet 2 of GrxC1; $\Delta E_Q = 0.66$ and $\delta = 0.27\,mm\,s^{-1}$ for doublet 1, and $\Delta E_Q = 0.94$ and $\delta = 0.32\,mm\,s^{-1}$ for doublet 2 of IscU.

residue in GrxS14 and S16. Three cysteine residues are present in GrxS14 at positions 33, 87 and 108 (recombinant poplar GrxS14 numbering). The active site cysteine (Cys33) is conserved in all CGFS Grxs. Cys87 is present in all S14- and S16-type plant Grxs, but not in S15-type plant Grxs, whereas Cys108 is even not conserved in all S14-type plant Grxs (Supplementary Figure 1). Hence, to address the cluster ligation in GrxS14 and check whether the inability for GrxS15 to incorporate a Fe–S cluster is a consequence of the absence of the second cysteine residue, cysteine mutants both on poplar and AtGrxS14 and on poplar GrxS15 have been generated. AtGrxS14 was used for these mutation studies because introducing these mutations in poplar GrxS14 led mostly to insoluble proteins. On the basis of the colour of the cells and supernatant following sonication and centrifugation, it was clear that AtGrxS14 C33S was no longer able to incorporate the cluster, whereas AtGrxS14 C87S, AtGrxS14 C108S and AtGrxS14 C87/108S were still able to incorporate it. Further confirmation that the second cysteine residue is not a ligand came from the observation that poplar GrxS15 S87C was still unable to accommodate a Fe–S cluster. Taken together, the mutagenesis and spectroscopic data, coupled with the requirement for GSH in cluster reconstitution experiments, strongly support similar cluster ligation in monothiol and dithiol Grxs (as typified by GrxS14 and GrxC1, respectively), involving the catalytic cysteine of two monomers and two external GSH molecules. The structural origin of the observed differences in spectroscopic properties of the $[2Fe–2S]^{2+}$ clusters in monothiol and dithiol Grxs is therefore likely to result from differences in ligand arrangement or cluster environment.

In vitro cluster transfer from [2Fe–2S] GrxS14 to apo chloroplast ferredoxin

The results presented above provide *in vitro* evidence in support of a role for monothiol Grxs as scaffolds for the assembly of [2Fe–2S] clusters. However, functional Fe–S

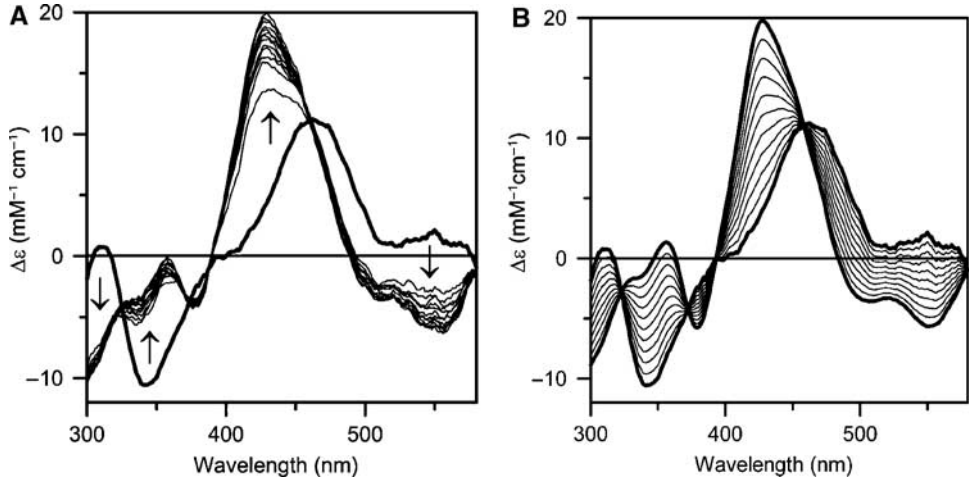

Figure 7 Time course of cluster transfer from poplar GrxS14 to apo *Synechocystis* Fd monitored by UV–visible CD spectroscopy at 23°C in 1 cm cuvettes. (**A**) CD spectra were recorded at 5-min intervals for a period of 60 min for a reaction mixture that was initially 15 μM in GrxS14 [2Fe–2S] clusters and 15 μM apo Fd. The spectrum at zero time (thick line) corresponds to [2Fe–2S] GrxS14 in the same reaction mixture in the absence of apo Fd. The arrows indicate the direction of intensity change with time at selected wavelengths. (**B**) Predicted changes in the CD spectra for quantitative cluster transfer. Thick lines correspond to holo forms of *Synechocystis* [2Fe–2S] Fd and [2Fe–2S] GrxS14 and thin lines correspond to simulated CD spectra corresponding to 10–90% [2Fe–2S] cluster transfer from GrxS14 to Fd in 10% increments. In both panels, Δε values are expressed per $[2Fe–2S]^{2+}$ cluster.

cluster scaffold proteins need to be capable both of assembling clusters and transferring them to apo forms of physiologically relevant acceptor proteins. We have therefore investigated the ability of [2Fe–2S] GrxS14, which is localized in chloroplasts, to transfer its cluster to an apo form of *Synechocystis* [2Fe–2S] ferredoxin, one of the most abundant and highly conserved of all chloroplastic Fe–S proteins.

Direct evidence for rapid and quantitative cluster transfer from [2Fe–2S] GrxS14 to apo Fd was provided by anaerobic CD studies as a function of time using a reaction mixture involving stoichiometric [2Fe–2S] GrxS14 and apo Fd (Figure 7). The marked difference in the CD spectra of $[2Fe–2S]^{2+}$ centres in GrxS14 and holo Fd in the reaction mixture facilitates direct monitoring of cluster transfer and assessment of the extent of intact cluster transfer via concomitant decrease and increase of the CD spectra of the cluster donor and acceptor, respectively. Comparison of the time course of CD changes in the reaction mixture (Figure 7A) with simulated data for 0–100% intact cluster transfer (Figure 7B) indicates quantitative cluster transfer from [2Fe–2S] GrxS14 to apo Fd that is 60% complete after 5 min and 100% complete after approximately 60 min. The agreement between the observed and simulated data and the rapid rate of Fd reconstitution suggests quantitative and intact cluster transfer from [2Fe–2S] GrxS14 to apo Fd and argues strongly against cluster degradation and reassembly of apo Fd. This conclusion is further supported by three additional pieces of evidence. First, absorption and CD studies of the reaction mixture in the absence of the apo Fd showed <10% degradation of the [2Fe–2S] cluster on GrxS14 after 60 min. Second, parallel CD studies of apo *Synechocystis* Fd reconstitution with equivalent amounts of S^{2-} and Fe^{3+} or Fe^{2+} under identical conditions resulted in $\sim$5% cluster assembly over a 60-min period. Third, the addition of 1 mM EDTA to the reaction mixture completely inhibited cluster reconstitution using S^{2-} and Fe^{3+} or Fe^{2+}, but had no significant effect on the time course of [2Fe–2S] GrxS14-mediated cluster assembly on apo Fd. Taken together, these observations indicate rapid, quantitative and intact cluster transfer from [2Fe–2S] GrxS14 to apo Fd. In contrast, parallel cluster transfer studies using the poplar dithiol [2Fe–2S] GrxC1 showed no indication of cluster transfer to apo *Synechocystis* Fd after 120 min (data not shown). Hence, the ability to transfer [2Fe–2S] clusters to acceptor proteins appears to be limited to monothiol Grxs. Comparative stability studies of GrxS14 and GrxC1 indicate that this is likely to be a consequence of increased accessibility and lability for the [2Fe–2S] clusters in monothiol Grxs compared with dithiol Grxs, see Supplementary Figure 2.

Quantitative assessment of the rate of cluster transfer as a function of [2Fe–2S] GrxS14 to apo Fd stoichiometry (0.22:1–1.5:1 based on cluster content of GrxS14) was obtained by continuous monitoring of the CD changes at 423 nm (Figure 8). On the basis of the initial concentrations of GrxS14 [2Fe–2S] clusters and apo Fd, the data in each case are well fit by second-order kinetics corresponding to stoichiometric cluster transfer with a rate constant of $20\,000\,M^{-1}\,min^{-1}$. To put this into context, the fastest intact [2Fe–2S] cluster transfer reported so far is for HscA/HscB/ATP-mediated [2Fe–2S] cluster transfer from [2Fe–2S] IscU to apo-IscFdx, which had a second-order rate constant of $800\,M^{-1}\,min^{-1}$ (Chandramouli and Johnson, 2006). Hence, the results demonstrate that [2Fe–2S] cluster transfer from [2Fe–2S] GrxS14 to apo Fd is stoichiometric, quantitative and occurs at a rate that is 25 × faster than *in vitro* cluster transfer studies using the IscU scaffold protein. Clearly these *in vitro* studies demonstrate that CGFS Grxs have the potential to function as scaffold proteins for the assembly and efficient delivery of [2Fe–2S] clusters.

Discussion

Involvement of chloroplastic CGFS Grxs in iron–sulphur cluster assembly

Grxs with a CGFS active site constitutes a recently described subgroup of the Grx family, whose functions are largely

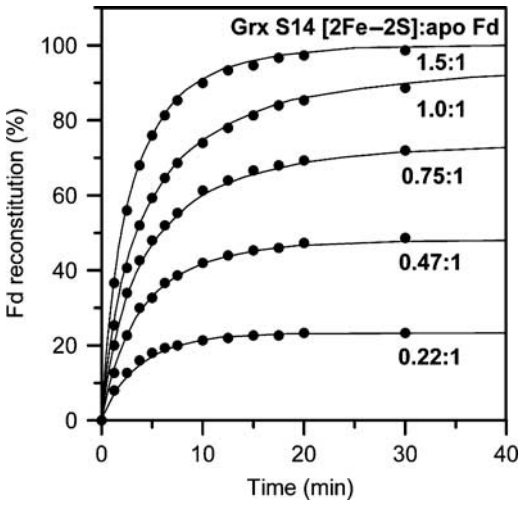

Figure 8 Kinetics of cluster transfer from poplar GrxS14 to apo *Synechocystis* Fd at 23°C as a function of the stoichiometry of GrxS14 [2Fe–2S] clusters to apo Fd. The experimental conditions are as described in Figure 7, except that the concentration of GrxS14 [2Fe–2S] clusters was varied to give the indicated GrxS14 [2Fe–2S] to apo Fd ratios. Reactions were continuously monitored using the CD intensity at 423 nm and converted to percent Fd reconstitution based on simulated data (as illustrated in Figure 7 for a 1:1 stoichiometry). Solid lines correspond to second-order kinetics with $k = 20\,000\,M^{-1}\,min^{-1}$ based on the initial concentrations of GrxS14 [2Fe–2S] clusters and apo Fd.

unknown at the present time (Herrero and de la Torre-Ruiz, 2007). In yeast, Grx5 was originally identified as playing a central role in protecting against oxidative damage and subsequent investigations refined a role in mitochondrial Fe–S cluster biogenesis (Rodríguez-Manzaneque *et al*, 1999, 2002). Immunoprecipitation studies suggested that Grx5 facilitates transfer of clusters assembled on the Isu scaffold protein to acceptor proteins (Mühlenhoff *et al*, 2003). In contrast, the other two CGFS Grxs in yeast, Grx3 and Grx4, are nuclear proteins involved in the nuclear localization regulation of the transcriptional iron regulators Aft1 and Aft2 (Ojeda *et al*, 2006). In plants, the CGFS Grx subgroup is expanded to four members, but the only functional information stems from *in vivo* analysis of *A. thaliana* GrxS14 (aka AtGRXcp), which was shown to be a chloroplastic protein probably involved in the oxidative stress response (Cheng *et al*, 2006).

In this study, the subcellular locations of each of the poplar CGFS Grxs were determined and yeast Δ*grx5* complementation studies of mitochondrial-targeted forms were used to assess the possibility that plant CGFS Grxs are also involved in Fe–S cluster assembly. All the CGFS Grxs, except GrxS15, but not dithiol Grxs (even GrxC1, which contains a [2Fe–2S] cluster), were able to complement the defects of the *yeast* Δ*grx5* mutant, although not always to a similar extent. These results were somewhat surprising because the two chloroplastic Grxs (GrxS14 and S16) are the most efficient proteins, whereas the mitochondrial GrxS15 is essentially not effective. In addition, the proteins involved in plant and yeast mitochondrial Fe–S cluster assembly belong to the ISC type of machinery, whereas plant chloroplasts contain essentially the SUF system. Nevertheless, it is evident that both GrxS14 and S16 have the ability to assume a role analogous to that of Grx5 in mitochondrial Fe–S cluster biosynthesis. Whether GrxS15 is involved in plant mitochondria Fe–S cluster assembly is still uncertain, but only one or two other Grxs, displaying a CCMS active site, are predicted to be present in mitochondria and could fulfil an analogous role. As discussed below, a major difference between GrxS14 or S16 and S15, that could explain their different behaviour, is the capacity of the two chloroplastic Grxs to incorporate a Fe–S cluster when expressed in *E. coli*.

GrxS14 and S16 as Fe–S cluster scaffold proteins

The observation that both plant GrxS14 and S16 contain analogous $[2Fe–2S]^{2+}$ centres when heterologously expressed in *E. coli* raises the possibility of a role for CGFS Grxs as scaffolds for the assembly of chloroplastic Fe–S clusters. Additional support for a scaffolding role comes from the ability to assemble spectroscopically identical clusters on apo GrxS14 in a cysteine desulphurase-mediated reaction in the presence of L-cysteine, Fe^{2+} ion and GSH. Cysteine mutagenesis studies, analytical and spectroscopic data, and the requirement of GSH to effect cluster assembly on apo GrxS14, indicate the presence of a subunit-bridging $[2Fe–2S]^{2+}$ cluster ligated by the first active site cysteine of two Grxs and the cysteines of two GSH molecules. A similar ligation has also been structurally established in the dithiol poplar GrxC1 (Rouhier *et al*, 2007). However, pronounced differences in the lability or accessibility and the ground-state vibrational and excited-state electronic properties of the [2Fe–2S] centres in monothiol and dithiol plant Grxs indicate differences in the cluster environment or the arrangement of coordinating cysteine residues. Possible differences could involve the extent and arrangement of aromatic residues in the vicinity of the cluster or *cis* rather than *trans* GSH cluster ligation (Rouhier *et al*, 2007). Crystallographic studies of cluster-bound forms of monothiol Grxs will be required to address these differences and to assess the cluster release mechanism in monothiol Grxs.

A functional Fe–S cluster scaffold protein must also be effective in transferring clusters to physiologically relevant acceptor proteins. Hence, the observation of rapid, stoichiometric and intact cluster transfer from [2Fe–2S] GrxS14 to apo Fd provides *in vitro* evidence for a role of CGFS Grxs as [2Fe–2S] cluster donors for maturation of chloroplast Fe–S proteins. In contrast, analogous cluster transfer experiments using the structurally characterized [2Fe–2S] cluster-bound dithiol GrxC1 failed to show any evidence of cluster transfer to apo Fd. Clearly, there is a pressing need to investigate the ability of [2Fe–2S] GrxS14 and [2Fe–2S] GrxS16 to effect maturation of the apo forms of a variety of [2Fe–2S] cluster-containing chloroplastic proteins, for example, sirohydrochlorin ferrochelatase, dihydroxyacid dehydratase and Rieske-type centres in oxygenases and the cytochrome b_6f, complex, and to assess the possibility that these proteins also participate in the maturation of [3Fe–4S] and [4Fe–4S] clusters in chloroplastic proteins. Such studies will address the specificity of these Grxs in chloroplastic Fe–S cluster biogenesis and are currently in progress in our laboratories. The proposed role for CGFS Grxs as Fe–S cluster scaffold proteins also provides a rationalization for the apparent disparity concerning the role of the second partly conserved cysteine residue in yeast Grx5 in *in vivo* and *in vitro* activity data. Mutagenesis results indicated that the second conserved cysteine is required for *in vitro* deglutathionylation activity, but is not required for *in vivo* Fe–S cluster biogenesis activity

(Belli *et al*, 2002) or the assembly of a [2Fe–2S] cluster on GrxS14. Nevertheless, among all natural or mutated plant CGFS Grxs tested, those which do not possess this additional cysteine (GrxS15 and GrxC4 CGFS) were not able to complement the *S. cerevisiae* Δ*grx5* mutant. This indicates that, although not essential for cluster incorporation, this additional cysteine may be required for an efficient complementation with plant Grxs.

Two pieces of evidence argue against a scaffolding role for monothiol CGFS Grxs in *de novo* Fe–S cluster assembly. First, gene disruptions of known chloroplastic scaffold proteins such as the Nfu proteins and other intrinsic components of the chloroplastic Fe–S assembly machinery are generally associated with a dwarf phenotype or abnormal development (Touraine *et al*, 2004; Yabe *et al*, 2004; Balasubramanian *et al*, 2006; Xu and Moller, 2006; Van Hoewyk *et al*, 2007). In the case of GrxS14, the phenotype consists of a defect in early seedling growth under oxidative stress (Cheng *et al*, 2006) and is not as strong as that associated with *nfu* gene disruptions. Taking into account the large number of Fe–S proteins in the chloroplast, one possibility is that GrxS14 has specific target proteins whose functions are not essential for plant development. Alternatively, the absence of GrxS14 may be compensated by other potential scaffold proteins such as GrxS16 or SufA in the loss-of-function mutant. To address this issue, it will be necessary to investigate the phenotypes of gene disruptions resulting in depletion of other chloroplast proteins, both individually and together, for example, GrxS16, GrxS14/GrxS16, SufA/GrxS14 and SufA/GrxS16. Second, the role of Grx5 in yeast mitochondrial Fe–S cluster biogenesis does not appear to be dependent on GSH, which is required for the assembly of a [2Fe–2S] cluster on GrxS14. Depletion of GSH was found to affect the maturation of cytosolic Fe–S proteins, but had no significant effect on mitochondrial Fe–S cluster biogenesis (Sipos *et al*, 2002). However, the significance of this observation remains to be established as there is currently no reliable information on the type of cluster or the requirements for cluster assembly on Grx5, or the level of GSH that is required to support mitochondrial Fe–S cluster assembly. A recent paper by Picciocchi *et al* (2007) reported *in vitro* assembly of a Fe–S cluster in yeast Grx5 and other CGFS Grxs in the presence of GSH. However, variability in the reported UV–visible absorption spectra, coupled with the absence of Mössbauer, CD, resonance Raman or quantitative EPR data, leaves the cluster content of these samples unresolved.

Alternative functions for monothiol CGFS Grxs

The ability of CGFS Grxs to accommodate [2Fe–2S] clusters and transfer them to acceptor proteins is also consistent with a role in storage of preformed Fe–S clusters or as Fe–S cluster delivery systems that mediate cluster transfer from other potential scaffold proteins (i.e. SufA, SufB and Nfu in chloroplasts and Isa/IscA, Nfu and Isu in mitochondria) to specific acceptor proteins. Such a role is consistent with yeast Δ*grx5* immunoprecipitation studies, which suggested that Grx5 facilitates transfer of clusters assembled on the Isu scaffold protein to acceptor proteins (Mühlenhoff *et al*, 2003). This would also explain why a strong phenotype may not be associated with gene disruption, because the transfer would still occur although at a lower rate. In addition, yeast two-hybrid studies indicate an *in vivo* interaction between Grx5 and Isa1 (Vilella *et al*, 2004) and the crystal structure of an IscA protein with an asymmetrical subunit-bridging [2Fe–2S] cluster has recently been published (Morimoto *et al*, 2006). Hence, it is possible that IscA/SufA-type proteins hand off clusters to monothiol Grxs for delivery to acceptor proteins and that this cluster assembly pathway would only be completely shut down by deletion of both genes. *In vitro* cluster transfer experiments involving chloroplast [2Fe–2S] SufA and [2Fe–2S] Nfu proteins and apo GrxS14 and kinetic studies of the effect on apo GrxS14 on the rates of cluster transfer from chloroplast [2Fe–2S] SufA and [2Fe–2S] Nfu to apo Fd are in progress to test this hypothesis.

In light of the proposed role for Grx3 and Grx4 in the regulation of Fe homeostasis in yeast (Ojeda *et al*, 2006), an alternative rationalization for the cluster-binding ability of chloroplast Grxs is that they play a role in the regulation of the SUF Fe–S cluster biogenesis machinery by facilitating assessment of the chloroplast Fe–S cluster status. Using bioinformatics, Huynen *et al* (2005) proposed that BolA proteins act as reductases that interact with monothiol Grxs in the oxidative stress response. Nevertheless, such a function seems unlikely in plants as BolA proteins do not possess conserved cysteines. Nevertheless, among the three genes encoding SufE proteins in *A. thaliana*, SufE1 (At4g26500) contains a C-terminal BolA domain (Xu and Moller, 2006; Ye *et al*, 2006a). SufE proteins are sulphur transferases that serve as activators for the NifS and SufS cysteine desulphurases in the initial steps of chloroplast Fe–S cluster biosynthesis (Xu and Moller, 2006). Hence, it is possible that GrxS14 acts as a Fe–S cluster-dependent regulator of the SUF machinery by interacting with SufE1 via the BolA domain. Under this scenario, Fe–S cluster incorporation into GrxS14 would occur under Fe–S cluster-replete conditions, resulting in enhanced interaction with SufE1 to limit the activity of the SUF Fe–S cluster biogenesis machinery.

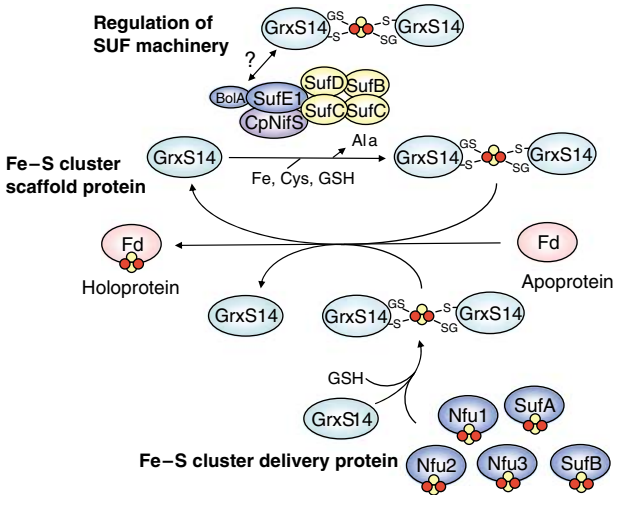

Figure 9 Working model for the potential roles of GrxS14 and S16 in chloroplastic Fe–S cluster assembly. GrxS14 and S16 could function as scaffold proteins for *de novo* synthesis and transfer of Fe–S clusters, as Fe–S cluster delivery proteins for mediating the transfer of Fe–S clusters from other potential scaffold proteins (Nfu1, 2 and 3, SufA and SufB) to acceptor proteins, or as regulators of the SUF machinery by interacting with the BolA domain of SufE1 in the cluster-bound form.

The three possible roles for CGFS Grxs in chloroplast Fe–S cluster biogenesis are summarized in Figure 9. It is important to emphasize that these three roles are not mutually exclusive and that all three could be operative in chloroplasts with GrxS14 and S16 having different specificity for acceptor proteins, cluster-donor proteins or cysteine desulfurases. Such functional variability and specificity differences may also be responsible for anomalous behaviour of GrxS15 and the truncated form of GrxS17 in yeast Grx5 complementation studies.

Materials and methods

Heterologous expression and purification of CGFS Grxs in E. coli

The cloning and aerobic purification procedures of CGFS Grxs are described as Supplementary data. Anaerobic purification of poplar GrxS14 and AtGrxS16 was carried out under Ar in a Vacuum Atmospheres glove box at oxygen levels <2 p.p.m. The cell pellet was resuspended in 100 mM Tris–HCl pH 8 with 1 mM GSH (buffer B), sonicated and centrifuged at 39 700 *g* for 1 h at 4°C to remove the cell debris. The reddish-brown cell-free extract containing holo GrxS14 was subjected to 40% ammonium sulphate cut followed by centrifugation. The brown pellet was resolubilized in buffer B and loaded onto a 10 ml Phenyl Sepharose column (GE Healthcare). The protein was eluted with a 1–0 M $(NH_4)_2SO_4$ gradient using buffer B. The purest fractions, as judged by SDS–PAGE analysis, were pooled and $(NH_4)_2SO_4$ was removed by ultrafiltration dialysis using a YM10 membrane and buffer B.

Reconstitution of a Fe–S cluster in apo poplar GrxS14

Reconstitution of poplar apo GrxS14, 0.4 mM in buffer B, was accomplished in a glove box under anaerobic conditions by incubating at room temperature for 150 min with 5 mM GSH, 2 mM DTT, 12-fold excess of Fe(II) (ferrous ammonium sulphate), L-cysteine and catalytic amounts of *E. coli* IscS (20 μM). Reagents in excess were removed by loading onto a High-Trap Q-Sepharose column (GE Healthcare) and eluting with a 0–1 M NaCl gradient in buffer B. The holo protein was eluted between 0.45 and 0.55 M NaCl and was desalted using ultrafiltration dialysis.

Yeast plasmids and strains

Grx sequences were cloned in-frame in the yeast plasmid pMM221, which contains the *S. cerevisiae* mitochondrial targeting sequence of Grx5 plus a C-terminal 3HA/His_6 tag, under the control of the doxycycline-regulatory $tetO_2$ promoter (Molina *et al*, 2004) (Table I). pMM54 (Rodríguez-Manzaneque *et al*, 2002) contains a yeast *GRX5-3HA* construction under its own promoter. *S. cerevisiae* strains are described in Table II. Plasmids were linearized by *Cla*I digestion previous to chromosomal integration.

Growth conditions for S. cerevisiae cells

S. cerevisiae cultures were grown as described in Molina *et al* (2004). Samples were taken from cultures grown exponentially for at least 10 generations at 30°C. Sensitivity to oxidants was determined onto YPD plates containing the indicated concentration of the agent, by spotting 1:5 serial dilutions of exponential cultures and recording growth after 2 days of incubation at 30°C.

Table I New plasmids employed in this study

Plasmids	Characteristics
pMM628	Sequence coding from amino acid 2–117 of GrxC1 cloned between *Not*I–*Pst*I sites of pMM221
pMM630	Sequence coding from amino acid 2–117 of GrxC1(G32P) cloned between *Not*I–*Pst*I sites of pMM221
pMM632	Sequence coding from amino acid 2–113 of GrxC4 cloned between *Not*I–*Pst*I sites of pMM221
pMM634	Sequence coding from amino acid 37–174 of GrxS15 cloned between *Not*I–*Pst*I sites of pMM221
pMM657	Sequence coding from amino acid 66–173 of GrxS14 cloned between *Not*I–*Pst*I sites of pMM221
pMM676	Derivative of pMM628 with the sequence coding for CGFS instead of CGYC in GrxC1
pMM712	Sequence coding from amino acid 85–296 of GrxS16 cloned between *Not*I–*Pst*I sites of pMM221
pMM713	Sequence coding from amino acid 1–492 of GrxS17 cloned between *Not*I–*Pme*I sites of pMM221
pMM714	Sequence coding from amino acid 398–492 of GrxS17 cloned between *Not*I–*Pme*I sites of pMM221

Table II Yeast strains employed in this study

Strains	Relevant phenotype	Comments
W303-1A	*MAT***a** *ura3-1 ade2-1 leu2-3,112 trp1-1 his3-11,15*	Wild type
W303-1B	As W303-1A but *MAT*α	Wild type
MML100	*MAT***a** *grx5*::*kanMX4*	Rodríguez-Manzaneque *et al* (2002)
MML240	*MAT***a** *grx5*::*kanMX4* [pMM54(*GRX5-3HA*)]::*LEU2*	Rodríguez-Manzaneque *et al* (2002)
MML755	*MAT*α [pMM628(*GrxC1-3HA*)]::*LEU2*	Integration of linear pMM628 in W303-1B
MML756	*MAT*α [pMM630($GrxC1_{G32P}$-*3HA*)]::*LEU2*	Integration of linear pMM630 in W303-1B
MML757	*MAT*α [pMM632(*GrxC4-3HA*)]::*LEU2*	Integration of linear pMM632 in W303-1B
MML758	*MAT*α [pMM634(*GrxS15-3HA*)]::*LEU2*	Integration of linear pMM634 in W303-1B
MML759	*MAT*α [pMM657(*GrxS14-3HA*)]::*LEU2*	Integration of linear pMM657 in W303-1B
MML761	*MAT***a** *grx5*::*kanMX4* [pMM628(*GrxC1-3HA*)]::*LEU2*	Spore from a cross MML100 × MML755
MML763	*MAT***a** *grx5*::*kanMX4* [pMM630($GrxC1_{G32P}$-*3HA*)]::*LEU2*	Spore from a cross MML100 × MML756
MML765	*MAT***a** *grx5*::*kanMX4* [pMM632(*GrxC4-3HA*)]::*LEU2*	Spore from a cross MML100 × MML757
MML767	*MAT***a** *grx5*::*kanMX4* [pMM634(*GrxS15-3HA*)]::*LEU2*	Spore from a cross MML100 × MML758
MML769	*MAT***a** *grx5*::*kanMX4* [pMM657(*GrxS14-3HA*)]::*LEU2*	Spore from a cross MML100 × MML759
MML779	*MAT*α [pMM676($GrxC1_{CGFS}$-*3HA*)]::*LEU2*	Integration of linear pMM676 in W303-1B
MML780	*MAT***a** *grx5*::*kanMX4* [pMM676($GrxC1_{CGFS}$-*3HA*)]::*LEU2*	Spore from a cross MML100 × MML779
MML786	*MAT*α [pMM712(*GrxS16-3HA*)]::*LEU2*	Integration of linear pMM712 in W303-1B
MML787	*MAT*α [pMM713(*GrxS17-3HA*)]::*LEU2*	Integration of linear pMM713 in W303-1B
MML788	*MAT*α [pMM714($GrxS17_{398-492}$-*3HA*)]::*LEU2*	Integration of linear pMM714 in W303-1B
MML806	*MAT***a** *grx5*::*kanMX4* [pMM712(*GrxS16-3HA*)]::*LEU2*	Spore from a cross MML100 × MML786
MML808	*MAT***a** *grx5*::*kanMX4* [pMM713(*GrxS17-3HA*)]::*LEU2*	Spore from a cross MML100 × MML787
MML810	*MAT***a** *grx5*::*kanMX4* [pMM714($GrxS17_{398-492}$-*3HA*)]::*LEU2*	Spore from a cross MML100 × MML788

Other methods

Mitochondria were purified and subfractionated (Diekert *et al*, 2001) from exponential yeast cultures in YPLactate medium at 30°C. Aconitase and malate dehydrogenase were assayed as described in Robinson *et al* (1987), in extracts prepared (Molina-Navarro *et al*, 2006) from cells growing exponentially in YPGalactose medium.

In vivo subcellular localization by GFP fusions

Full-length open reading frames were cloned in 5′ of the GFP sequence under the control of a double 35S promoter into the plasmid pCK S65C between *Nco*I and *Bam*HI sites (underlined) using primers described in Supplementary Table I. *Nicotiana benthamiana* cells were transfected by bombardment of leaves with tungsten particles coated with plasmid DNA and images were obtained with a Zeiss LSM510 confocal microscope.

Analytical and spectroscopic methods

Protein concentrations were determined by the *DC* protein assay (Bio-Rad), using BSA as a standard. Iron concentrations were determined using bathophenanthroline under reducing conditions, after digestion of the protein in 0.8% $KMnO_4$/0.2 M HCl (Fish, 1988). Sample concentrations and extinction coefficients are based on protein monomer and samples were in 100 mM Tris–HCl pH 8 with 1 mM GSH, unless indicated otherwise. Samples for spectroscopic studies were prepared under Ar in a Vacuum Atmospheres glove box ($O_2 < 2$ p.p.m.). UV–visible absorption and CD spectra were recorded at room temperature using a Shimadzu UV-3101PC spectrophotometer and Jasco J-715 spectropolarimeter, respectively. Resonance Raman spectra were recorded as previously described (Cosper *et al*, 2004), using an Instruments SA Ramanor U1000 spectrometer coupled with a Coherent Sabre argon ion laser, with 20 µl frozen droplets of 2–3 mM sample mounted on the cold finger of an Air Products Displex Model CSA-202E closed cycle refrigerator. Mössbauer spectra were recorded by using the previously described instrumentations (Ravi *et al*, 1994). The zero velocity of the spectra refers to the centroid of a room temperature spectrum of a metallic Fe foil. Analysis of the Mössbauer data was performed with the WMOSS program (Web Research).

Fe–S cluster transfer experiments

Synechocystis Fd for cluster transfer experiments was heterologously expressed in *E. coli* and purified according to published procedures (Glauser *et al*, 2004). Apo Fd was prepared by treating the holo protein with EDTA and potassium ferricyanide at room temperature under anaerobic conditions and removing excess reagents by ultrafiltration dialysis using a YM10 membrane and buffer B. The time course of cluster transfer from [2Fe–2S] GrxS14 to apo Fd was monitored under anaerobic conditions in 1 cm cuvettes at 23°C using UV–visible CD spectroscopy. The reactions were carried out in buffer B with 5 mM DTT and apo Fd was added 60 min prior to initiation of the cluster transfer reactions by addition of [2Fe–2S] GrxS14. Changes in the CD spectra at 423 nm were used to assess the concentration of holo Fd formed as a function of time. The time course of holo Fd formation was analysed by fitting to second-order kinetics, based on the initial concentrations of GrxS14 [2Fe–2S] clusters and apo-Fd in the reaction mixture, using the Chemical Kinetics Simulator software package (IBM).

Supplementary data

Supplementary data are available at *The EMBO Journal* Online (http://www.embojournal.org).

Acknowledgements

This research was supported by grants from the National Institutes of Health (GM62524 to MKJ and GM47295 to BHH), from BFU2004-03167 (Ministerio de Educación y Ciencia) and 2005SGR-00677 (Generalitat de Catalunya) to EH and from the ANR programs (GNP05010G and JC07_204825) to NR, FG and JPJ.

References

Achebach S, Tran QH, Vlamis-Gardikas A, Mullner M, Holmgren A, Unden G (2004) Stimulation of Fe–S cluster insertion into apoFNR by *E. coli* glutaredoxins 1, 2 and 3 *in vitro*. *FEBS Lett* **565:** 203–206

Agar JN, Krebs B, Frazzon J, Huynh BH, Dean DR, Johnson MK (2000) IscU as a scaffold for iron–sulfur cluster biosynthesis: sequential assembly of [2Fe–2S] and [4Fe–4S] clusters in IscU. *Biochemistry* **39:** 7856–7862

Balasubramanian R, Shen G, Bryant DA, Golbeck JH (2006) Regulatory roles for IscA and SufA in iron homeostasis and redox stress responses in the cyanobacterium *Synechococcus* sp. strain PCC 7002. *J Bacteriol* **88:** 3182–3191

Balk J, Lobreaux S (2005) Biogenesis of iron–sulfur proteins in plants. *Trends Plant Sci* **10:** 324–331

Belli G, Polaina J, Tamarit J, De La Torre MA, Rodriguez-Manzaneque MT, Ros J, Herrero E (2002) Structure–function analysis of yeast Grx5 monothiol glutaredoxin defines essential amino acids for the function of the protein. *J Biol Chem* **277:** 37590–37596

Chandramouli K, Johnson MK (2006) HscA and HscB stimulate [2Fe–2S] cluster transfer from IscU to apoferredoxin in an ATP-dependent reaction. *Biochemistry* **45:** 11087–11095

Chandramouli K, Unciuleac M-C, Naik S, Dean DR, Huynh BH, Johnson MK (2007) Formation and properties of [4Fe–4S] clusters on the IscU scaffold protein. *Biochemistry* **46:** 6804–6811

Cheng NH, Liu JZ, Brock A, Nelson RS, Hirschi KD (2006) AtGRXcp, an *Arabidopsis* chloroplastic glutaredoxin, is critical for protection against protein oxidative damage. *J Biol Chem* **281:** 26280–26288

Cosper MM, Krebs C, Hernandez H, Jameson GNL, Eidsness MK, Huynh BH, Johnson MK (2004) Characterization of the cofactor content of *Escherichia coli* biotin synthase. *Biochemistry* **43:** 2007–2021

Dailey HA, Finnegan MG, Johnson MK (1994) Human ferrochelatase is an iron–sulfur protein. *Biochemistry* **33:** 403–407

Diekert K, de Kroon AIPM, Kispal G, Lill R (2001) Isolation and subfractionation of mitochondria from the yeast *Saccharomyces cerevisiae*. *Methods Cell Biol* **65:** 37–51

Feng Y, Zhong N, Rouhier N, Hase T, Kusunoki M, Jacquot JP, Jin C, Xia B (2006) Structural insight into poplar glutaredoxin C1 with a bridging iron–sulfur cluster at the active site. *Biochemistry* **45:** 7998–8008

Fish WW (1988) Rapid colorimetric micromethod for the quantitation of complexed iron in biological samples. *Methods Enzymol* **158:** 357–364

Fu W, Drozdzewski PM, Davies MD, Sligar SG, Johnson MK (1992) Resonance Raman and magnetic circular dichroism studies of reduced [2Fe–2S] proteins. *J Biol Chem* **267:** 15502–15510

Gelling C, Dawes IA, Richhardt N, Lill R, Mühlenhoff U (2008) Mitochondrial Iba57p is required for Fe/S cluster formation on aconitase and activation of radical SAM enzymes. *Mol Cell Biol* **28:** 1851–1861

Glauser DA, Bourquin F, Manieri W, Schürmann P (2004) Characterization of ferredoxin:thioredoxin reductase modified by site-directed mutagenesis. *J Biol Chem* **279:** 16662–16669

Han S, Czernuszewicz RS, Kimura T, Adams MWW, Spiro TG (1989) Fe_2S_2 protein resonance Raman revisited: structural variations among adrenodoxin, ferredoxin, and red paramagnetic protein. *J Am Chem Soc* **111:** 3505–3511

Herrero E, de la Torre-Ruiz MA (2007) Monothiol glutaredoxins: a common domain for multiple functions. *Cell Mol Life Sci* **64:** 1518–1530

Huynen MA, Spronk CA, Gabaldon T, Snel B (2005) Combining data from genomes, Y2H and 3D structure indicates that BolA is a reductase interacting with a glutaredoxin. *FEBS Lett* **579:** 591–596

Johansson C, Kavanagh KL, Gileadi O, Oppermann U (2007) Reversible sequestration of active site cysteines in a 2Fe–2S-bridged dimer provides a mechanism for glutaredoxin 2 regulation in human mitochondria. *J Biol Chem* **282:** 3077–3082

Johnson DC, Dean DR, Smith AD, Johnson MK (2005) Structure, function, and formation of biological iron–sulfur clusters. *Annu Rev Biochem* **74:** 247–281

Johnson MK, Smith AD (2005) Iron–sulfur proteins. In *Encyclopedia of Inorganic Chemistry*, King RB (ed), 2nd edn, pp 2589–2619. Chichester, UK: John Wiley & Sons

Layer G, Gaddam SA, Ayala-Castro CN, Ollagnier-de Choudens S, Lascoux D, Fontecave M, Outten FW (2007) SufE transfers sulfur from SufS to SufB for iron–sulfur cluster assembly. *J Biol Chem* **282:** 13342–13350

Lill R, Mühlenhoff U (2005) Iron–sulfur-protein biogenesis in eukaryotes. *Trends Biochem Sci* **30:** 133–141

Lillig CH, Berndt C, Vergnolle O, Lonn ME, Hudemann C, Bill E, Holmgren A (2005) Characterization of human glutaredoxin 2 as iron–sulfur protein: a possible role as redox sensor. *Proc Natl Acad Sci USA* **102:** 8168–8173

Molina MM, Bellí G, de la Torre MA, Rodríguez-Manzaneque MT, Herrero E (2004) Nuclear monothiol glutaredoxins of *S. cerevisiae* can function as mitochondrial glutaredoxins. *J Biol Chem* **279:** 51923–51930

Molina-Navarro MM, Casas C, Piedrafita L, Bellí G, Herrero E (2006) Prokaryotic and eukaryotic monothiol glutaredoxins are able to perform the functions of Grx5 in the biogenesis of Fe/S clusters in yeast mitochondria. *FEBS Lett* **580:** 2273–2280

Morimoto K, Yamashita E, Kondou Y, Lee SJ, Arisaka F, Tsukihara T, Nakai M (2006) The asymmetric IscA homodimer with an exposed [2Fe–2S] cluster suggests the structural basis of the Fe–S cluster biosynthetic scaffold. *J Mol Biol* **360:** 117–132

Mühlenhoff U, Gerber J, Richhardt N, Lill R (2003) Components involved in assembly and dislocation of iron–sulfur clusters on the scaffold protein Isu1p. *EMBO J* **22:** 4815–4825

Ojeda L, Keller G, Mühlenhoff U, Rutherford JC, Lill R, Winge DR (2006) Role of glutaredoxin-3 and glutaredoxin-4 in the iron regulation of the Aft1 transcriptional activator in *S. cerevisiae*. *J Biol Chem* **281:** 17661–17669

Picciocchi A, Saguez C, Boussac A, Cassier-Chauvat C, Chauvat F (2007) CGFS-type monothiol glutaredoxins from the cyanobacterium *Synechocystis* PCC6803 and other evolutionary distant model organisms possess a glutathione-ligated [2Fe–2S] cluster. *Biochemistry* **46:** 15018–15026

Ravi N, Bollinger JM, Huynh BH, Edmondson DE, Stubbe J (1994) Mechanism of assembly of the tyrosyl radical-diiron(III) cofactor of *E. coli* ribonucleotide reductase. 1. Mössbauer characterization of the diferric radical precursor. *J Am Chem Soc* **116:** 8007–8014

Robinson Jr JB, Brent LG, Sumegi B, Srere PA (1987) An enzymatic approach to the study of the Krebs tricarboxylic acid cycle. In *Mitochondria: a Practical Approach*, Darley-Usmar WM, Rickwood D, Wilson MT (eds), pp 153–170. Oxford, UK: IRL Press

Rodríguez-Manzaneque MT, Ros J, Cabiscol E, Sorribas A, Herrero E (1999) Grx5 glutaredoxin plays a central role in protection against protein oxidative damage in *S. cerevisiae*. *Mol Cell Biol* **19:** 8180–8190

Rodríguez-Manzaneque MT, Tamarit J, Bellí G, Ros J, Herrero E (2002) Grx5 is a mitochondrial glutaredoxin required for the activity of iron/sulfur clusters. *Mol Biol Cell* **13:** 1109–1121

Rouhier N, Gelhaye E, Jacquot JP (2004) Plant glutaredoxins: still mysterious reducing systems. *Cell Mol Life Sci* **61:** 1266–1277

Rouhier N, Unno H, Bandyopadhyay S, Masip L, Kim SK, Hirasawa M, Gualberto JM, Lattard V, Kusunoki M, Knaff DB, Georgiou G, Hase T, Johnson MK, Jacquot JP (2007) Functional, structural and spectroscopic characterization of a glutathione-ligated [2Fe−2S] cluster in poplar glutaredoxin C1. *Proc Natl Acad Sci USA* **104:** 7379–7384

Sipos K, Lange H, Fekete Z, Ullmann P, Lill R, Kispal G (2002) Maturation of cytosolic iron–sulfur proteins requires glutathione. *J Biol Chem* **277:** 26944–26949

Stephens PJ, Thomson AJ, Dunn JBR, Keiderling TA, Rawlings J, Rao KK, Hall DO (1978) Circular dichroism and magnetic circular dichroism of iron–sulfur proteins. *Biochemistry* **17:** 4770–4778

Tamarit J, Bellí G, Cabiscol E, Herrero E, Ros J (2003) Biochemical characterization of yeast mitochondrial Grx5 monothiol glutaredoxin. *J Biol Chem* **278:** 25745–25751

Touraine B, Boutin JP, Marion-Poll A, Briat JF, Peltier G, Lobreaux S (2004) Nfu2: a scaffold protein required for [4Fe–4S] and ferredoxin iron–sulfur cluster assembly in *Arabidopsis* chloroplasts. *Plant J* **40:** 101–111

Van Hoewyk D, Abdel-Ghany SE, Cohu CM, Herbert SK, Kugrens P, Pilon M, Pilon-Smits EA (2007) Chloroplast iron–sulfur cluster protein maturation requires the essential cysteine desulfurase CpNifS. *Proc Natl Acad Sci USA* **104:** 5686–5691

Vilella F, Alves R, Rodríguez-Manzaneque MT, Bellí G, Swaminathan S, Sunnerhagen P, Herrero E (2004) Evolution and cellular function of monothiol glutaredoxins: involvement in iron–sulfur cluster assembly. *Comp Funct Genom* **5:** 328–341

Wingert RA, Galloway JL, Barut B, Foott H, Fraenkel P, Axe JL, Weber GJ, Dooley K (2005) Deficiency of glutaredoxin 5 reveals Fe–S clusters are required for vertebrate haem synthesis. *Nature* **436:** 1035–1039

Xu XM, Moller SG (2006) AtSufE is an essential activator of plastidic and mitochondrial desulfurases in *Arabidopsis*. *EMBO J* **25:** 900–909

Yabe T, Morimoto K, Kikuchi S, Nishio K, Terashima I, Nakai M (2004) The *Arabidopsis* chloroplastic NifU-like protein CnfU, which can act as an iron–sulfur cluster scaffold protein, is required for biogenesis of ferredoxin and photosystem I. *Plant Cell* **16:** 993–1007

Ye H, Abdel-Ghany SE, Anderson TD, Pilon-Smits EA, Pilon M (2006a) CpSufE activates the cysteine desulfurase CpNifS for chloroplastic Fe–S cluster formation. *J Biol Chem* **281:** 8958–8969

Ye H, Pilon M, Pilon-Smits EA (2006b) CpNifS-dependent iron–sulfur cluster biogenesis in chloroplasts. *New Phytol* **171:** 285–292